Human Cancer Biology

Clinical Cancer Research

A NOTCH3 Transcriptional Module Induces Cell Motility in Neuroblastoma

Johan van Nes, Alvin Chan, Tim van Groningen, Peter van Sluis, Jan Koster, and Rogier Versteeg

Abstract

Purpose: Neuroblastoma is a childhood tumor of the peripheral sympathetic nervous system with an often lethal outcome due to metastatic disease. Migration and epithelial–mesenchymal transitions have been implicated in metastasis but they are hardly investigated in neuroblastoma.

Experimental Design: Cell migration of 16 neuroblastoma cell lines was quantified in Transwell migration assays. Gene expression profiling was used to derive a migration signature, which was applied to classify samples in a neuroblastoma tumor series. Differential expression of transcription factors was analyzed in the subsets. NOTCH3 was prioritized, and inducible transgene expression studies in cell lines were used to establish whether it functions as a master switch for motility.

Results: We identified a 36-gene expression signature that predicts cell migration. This signature was used to analyse expression profiles of 88 neuroblastoma tumors and identified a group with distant metastases and a poor prognosis. This group also expressed a known mesenchymal gene signature established in glioblastoma. Neuroblastomas recognized by the motility and mesenchymal signatures strongly expressed genes of the NOTCH pathway. Inducible expression of a NOTCH intracellular (*NOTCH3-IC*) transgene conferred a highly motile phenotype to neuroblastoma cells. NOTCH3-IC strongly induced expression of motility- and mesenchymal marker genes. Many of these genes were significantly coexpressed with NOTCH3 in neuroblastoma, as well as colon, kidney, ovary, and breast tumor series.

Conclusion: The NOTCH3 transcription factor is a master regulator of motility in neuroblastoma. A subset of neuroblastoma with high expression of NOTCH3 and its downstream-regulated genes has mesenchymal characteristics, increased incidence of metastases, and a poor prognosis. *Clin Cancer Res; 19(13); 3485–94. ©2013 AACR.*

Introduction

Neuroblastoma is a childhood tumor with a highly variable clinical outcome, ranging from spontaneous tumor regression to progression with distant metastasis despite aggressive multimodal therapy (reviewed in ref. 1). The tumor originates from the peripheral sympathetic nervous lineage, which is derived from the neural crest (2). Accordingly, neuroblastoma express markers of the developing peripheral sympathetic nervous system like, for example, PHOX2B, DBH, and TH (3). Early neural crest cells develop at the border between neural and non-neural ectoderm under the influence of Wnt, BMP, fibroblast growth factor, and Notch signaling pathways (reviewed in ref. 4). After an epithelial-to-mesenchymal transition (EMT), neural crest cells delaminate from the neural tube and start migrating throughout the body (2). Ultimately, migrating neural crest cells undergo a mesenchymal-to-epithelial transition and differentiate into a wide variety of cell types, depending on their final localization in the embryo. Reminiscent of the migratory phase of neuroblasts during normal development, high-stage neuroblastoma is characterized by local invasion of lymph nodes and metastasis to bone and bone marrow (5). These tumors have a poor prognosis in contrast to low-stage neuroblastomas that are not or only locally invasive and have an excellent prognosis.

Gene expression profiling has identified a mesenchymal subtype in glioblastoma brain tumors (6, 7). This mesenchymal state can be induced by combined expression of CAAT/enhancer-binding protein β and STAT3 transcription factors or the transcriptional coactivator, TAZ, which confers tumor-initiating and invasive phenotypes (8, 9). Also in small cell lung cancer (SCLC), overexpression of constitutively active RAS can induce mesenchymal features in the neuroendocrine cells (10). Thus, tumor cells of neuronal and epithelial origin can switch cell fates along an aberrant mesenchymal lineage (6, 10). Although neuroblastoma is widely metastatic, the molecular mechanisms driving dissemination and their relationship to migration and EMT

Authors' Affiliation: Department of Oncogenomics, Academic Medical Center, Amsterdam, the Netherlands

Note: Supplementary data for this article are available at Clinical Cancer Research Online (http://clincancerres.aacrjournals.org/).

Corresponding Author: Johan van Nes, Department of Oncogenomics, Academic Medical Center, Meibergdreef 9, P.O. box 1105 AZ Amsterdam, the Netherlands. Phone: 31-20-566-5170; Fax: 31-20-691-8626; E-mail: W.J.vannes@amc.uva.nl

doi: 10.1158/1078-0432.CCR-12-3021

Translational Relevance

Cell migration and invasion are crucial steps in the metastatic behavior of cancer cells. Aggressive neuroblastomas are characterized by distant metastases to the bone and bone marrow. In this study, we identified a group of neuroblastoma tumors with a mesenchymal gene expression profile and increased frequency of metastases. These tumors have increased expression of NOTCH pathway genes. Cell line analyses showed that NOTCH3 intracellular (NOTCH3-IC) induced a highly motile phenotype as well as strong regulation of cell motility- and mesenchymal marker genes. These analyses identify NOTCH3 as a master regulator of a migratory phenotype *in vitro* and prioritize this pathway for therapeutic targeting in neuroblastoma.

remain enigmatic. Intriguingly, breast cancer research showed an intimate relationship between stemness of cancer cells and EMT (11, 12).

The Notch signaling pathway controls cell fate decisions in a wide variety of cell types, including the nervous system (reviewed in ref. 13). NOTCH receptors are activated by ligands of the DELTA or JAGGED families on adjacent cells, resulting in their proteolytic cleavage and the translocation of the NOTCH intracellular domain (NOTCH-IC) into the nucleus. The NOTCH-IC forms a transcriptional activation complex with MAML proteins to drive transcription of target genes (14).

Here, we studied migration as a functional hallmark of a mesenchymal phenotype in neuroblastoma cell lines and tumors. Gene expression profiling identified a 36-gene mRNA expression signature associated with a migratory phenotype. This migration signature identified a mesenchymal state in neuroblastoma and glioblastoma tumors, correlating with increased metastatic incidence and poor prognosis. We identify NOTCH3 as a master switch-driving expression of cell motility- and mesenchymal marker genes, resulting in strong induction of neuroblastoma cell motility. Finally, a coregulated set of NOTCH3 target genes was observed in many tumor types.

Materials and Methods

Cell culture and generation of inducible NOTCH3-IC cell lines

Cell lines were cultured in Dulbecco's modified Eagle medium (DMEM; Gibco), supplemented with 10% fetal calf serum (FCS; Gibco), 1× nonessential amino acids (Gibco), 2 mmol/L L-glutamine (Gibco), and 10 U penicilline/10 μg streptomycine (Sigma) per mL. IMR32 cells with inducible overexpression of NOTCH3-IC were generated using the "Tet-on" expression system of Invitrogen. An IMR32-pcDNA6/TR subclone (repressing the Tet promoter) was transfected with an inducible pcDNA4/TO-NOTCH3-IC construct. Single-cell derived clones (clone 6 and clone 8) yielded IMR32 cell lines that drive expression of the NOTCH3-IC transgene in the presence of 50 ng/mL doxycycline as verified by Northern and Western blot analyses. Primary antibodies used were Notch3 (M-20, Santa Cruz Biotechnology; 1:1000 dilution; D11B8, Cell Signaling; 1:1000) and β-actin (Sigma, 1:20.000 dilution). Secondary horseradish peroxidase -conjugated anti-mouse (GE healthcare), anti-rat (GE healthcare) antibodies were incubated in 5% Non-fat Dry Milk/PBS for 1 hour at room temperature.

Gene expression profiling and analysis of microarray data

Total RNA from cultured cell lines as well as from 2 independent IMR32-TR6-NOTCH3-IC clones (clones 6 and 8) at various time-points after NOTCH3-IC induction was isolated using Trizol reagent (Invitrogen) according to the manufacturers' instructions. RNA quality of 28S and 18S ribosomal bands was verified on a BioAnalyzer (Agilent). RNA was hybridized on Affymetrix HG U133A plus2.0 gene chips and scanned data were normalized using the MASS5.0 algorithm. Expression data are stored in the R2 bioinformatics program and available from our public accessible website (http://R2.amc.nl). Bioinformatic analysis of microarray data was conducted with the R2 tool and TMeV v4.6.1 (30, 31).

Two groups of cell lines with high (SKNAS, SJNB8, SH-EP2) and low migration indices (SKNFI, IMR32, SJNB10, NMB, CHP134, SKNSH, NGP, KCNR, TR14, LAN5, LAN1, SY5Y, SJNB6) were generated with the custom track function. Differentially expressed genes were identified by ANOVA on ^{2}log-transformed gene expression values in groups of cell lines with high and low migration indices using a P value cutoff of $P < 0.01$ and a FDR correction for multiple testing. A minimum of 1 present call was required.

After informed consent, neuroblastoma tumor biopsies were collected from a total of 88 patients before initiation of treatment. Patients are treated according to the NCOG2009 protocol. A detailed description of tumor samples, clinical annotation, mRNA isolation, and gene expression profiling will be published elsewhere (Koster and colleagues; submitted for publication). Microarray data are available from the R2 website (http://R2.amc.nl) and from Gene Expression Omnibus (accession numbers GSM414091-GSM414107).

Transwell migration assay

Thirty-thousand cells were seeded in DMEM without FCS in polycarbonate Transwell inserts with 8 μmol/L pores (Costar). One-thousand IMR32-NOTCH3-IC cells were seeded in 12-well Transwell inserts (Greiner BioOne) and allowed to migrate for 72 hours. DMEM containing 10% FCS was used as a chemo attractant. After 24 hours, nonmigrated cells were removed from the top chamber using a cotton swab. Migrated cells were washed in PBS, fixed in 50% methanol/PBS followed by 100% methanol, and stained with 0.5% crystal violet in methanol. Experiments were quantified by counting digital images (× 200 magnification) of 4 independent and representative fields of migrated cells on a Leica inverted

microscope. Experiments were carried out in triplicate and repeated at least 2 times.

Wound-healing assay

Confluent cells were wounded using a yellow pipette tip. Triplicate wounds were made, washed, and further cultured in DMEM with 0.1% FCS. Assays were repeated 3 times for each IMR32-NOTCH3-IC clone.

Time-lapse video microscopy

Sparsely seeded IMR32-NOTCH3-IC cells were induced with doxycycline for 24 hours, followed by time-lapse photo microscopy at 10-minute intervals for 24 hours. Metamorph software (Universal Imaging) was used to take phase-contrast images.

Results

Characterization of neuroblastoma cell migration

A crucial step in metastatic behavior of cancer cells is the acquisition of migratory and invasive capacity (reviewed in ref. 15). The molecular circuitry that controls migration in neuroblastoma is largely unknown. To characterize a migratory state in neuroblastoma, we quantified migratory capacity of neuroblastoma cell lines in a Boyden chamber migration assay *in vitro*. A migration index was determined for a panel of 16 neuroblastoma cell lines (Fig. 1A). Using the average migration index of 22.5 as a cutoff, 3 cell lines migrated relatively faster as opposed to 13 other cell lines (Student t test; $P < 0.001$; Fig. 1A). We hereafter refer to these cell lines as groups with high and low migration, respectively.

A 36-gene expression signature predicts cell migration

Certain phenotypic characteristics of cells or tissues are associated with an underlying mRNA expression signature (e.g., refs. 16, 17). To identify a mRNA expression signature associated with migration, we conducted gene expression profiling of the 16 neuroblastoma cell lines using Affymetrix HG U133 Plus2.0 arrays. Analysis of differentially expressed genes between the groups with high and low migration identified 37 genes, 13 upregulated and 24 downregulated in cell lines with high migration [ANOVA; $P < 0.01$; false discovery rate (FDR)-corrected; Fig. 1B and Supplementary Table S1]. We removed one gene from this signature (LOC149773), as it was not significantly expressed in a series of 88 neuroblastoma tumors (see below). Literature mining revealed an experimentally proven function in cell

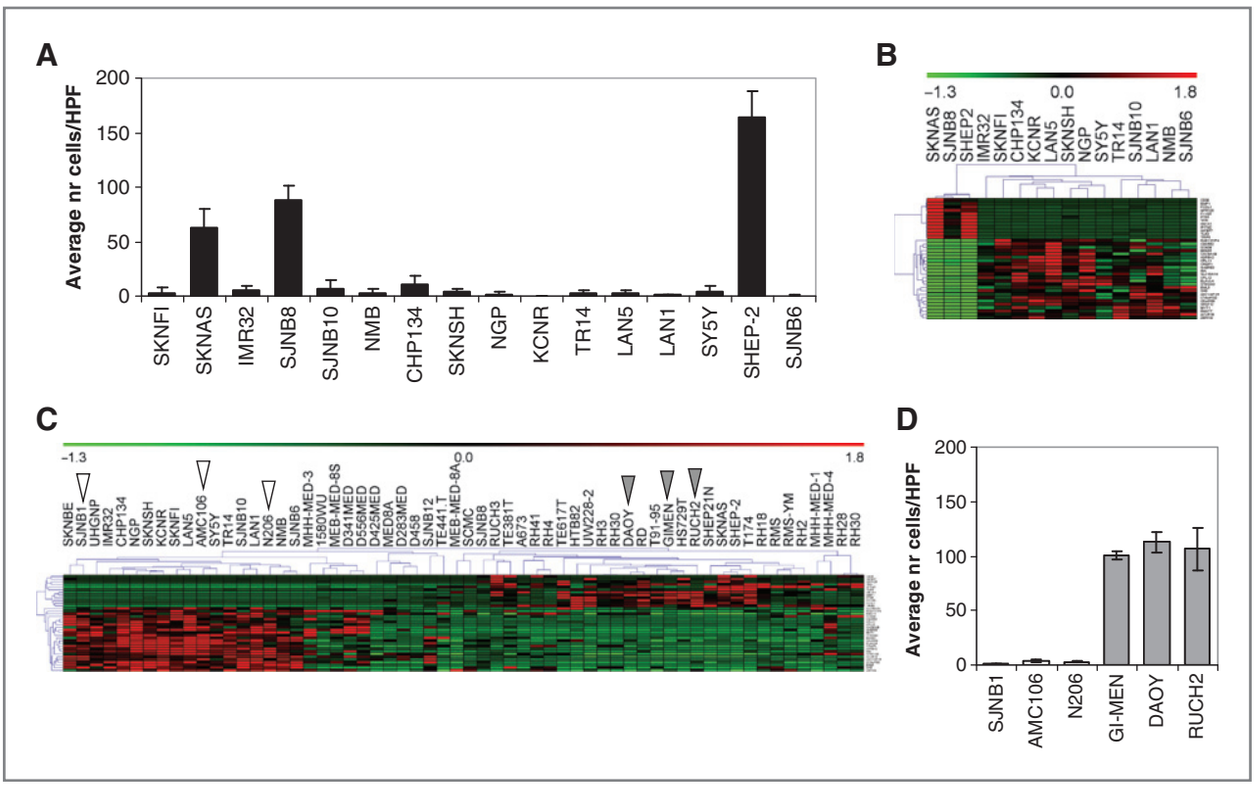

Figure 1. Identification of a 36-gene migration signature. A, Transwell migration assay for 16 different neuroblastoma cell lines. Histograms represent the average number (nr) of migrated cells from 2 independent experiments carried out in triplicate. Error bars indicate SD. B, heatmap showing differential expression of 36 genes between groups of cell lines with high and low migration indices. C, heatmap visualization of unsupervised cluster analysis of the 36-gene chemotaxis signature in a panel of neuroblastoma, medulloblastoma, and rhabdomyosarcoma cell lines. Open and filled arrowheads indicate cell lines with predicted low and high migration indices, respectively. D, migration assay of cell lines with predicted low (SJNB1, AMC106, N206, white bars) and high migration indices (GIMEN, DAOY, and RUCH2, grey bars).

migration, invasion, and/or metastasis for 13 of the remaining 36 genes. For instance, FXYD5 (Dysadherin) promotes metastasis of liver and pancreatic cancer cells (18, 19), and ANXA1 (Annexin A1) promotes TGFβ-dependent metastasis of basal-like breast cancer cells (20).

The robustness of the 36-gene signature was validated by predicting the migration phenotype of other cancer cell lines. We analyzed the 36-gene signature in a combined set of 14 medulloblastoma, 22 rhabdomyosarcoma, and 24 neuroblastoma cell lines, including the 16 neuroblastoma cell lines originally tested. Two-way hierarchical cluster analysis showed that cell lines SJNB1, N206, and AMC106 clustered with low migratory cell lines, whereas cell lines GI-MEN, DAOY, and RUCH2 clustered with high migratory cells (Fig. 1C). Analysis of these 6 cell lines in Transwell migration assays confirmed a high migration index for GI-MEN, DAOY, and RUCH2, whereas SJNB1, AMC106, and N206 hardly migrated (Fig. 1D). A scratch assay for cell migration revealed that fast migrating lines displayed efficient wound closure as opposed to slow migrating lines (Supplementary Fig. S1). We conclude that the 36-gene signature correctly assigns a migratory phenotype across different tumor genetic backgrounds.

The migration signature marks metastatic neuroblastoma with mesenchymal characteristics

As high-stage neuroblastoma is widely metastasized and motility is one of the requirements for the multistep process of metastasis, we tested the migration signature in a series of 88 primary neuroblastoma tumors (AMC-NB88) and analyzed the relationship with metastasis and survival (Summary information for AMC-NB88 in Supplementary Table S2; Koster and colleagues; submitted for publication). We classified the tumor series by K-means clustering in 3 groups, with a low (cluster 1), intermediate (cluster 2), and high (cluster 3) expression of the signature (Fig. 2A and Supplementary Table S3). The clustering was repeated 100 times to select the clustering with the lowest distance to the mean. This process was repeated 10 times (total 10 times 100 clusterings), allowing evaluation of the consistency of the 10 outcomes. This showed that the obtained classification was robust (displayed in Fig. 2A). The coregulated

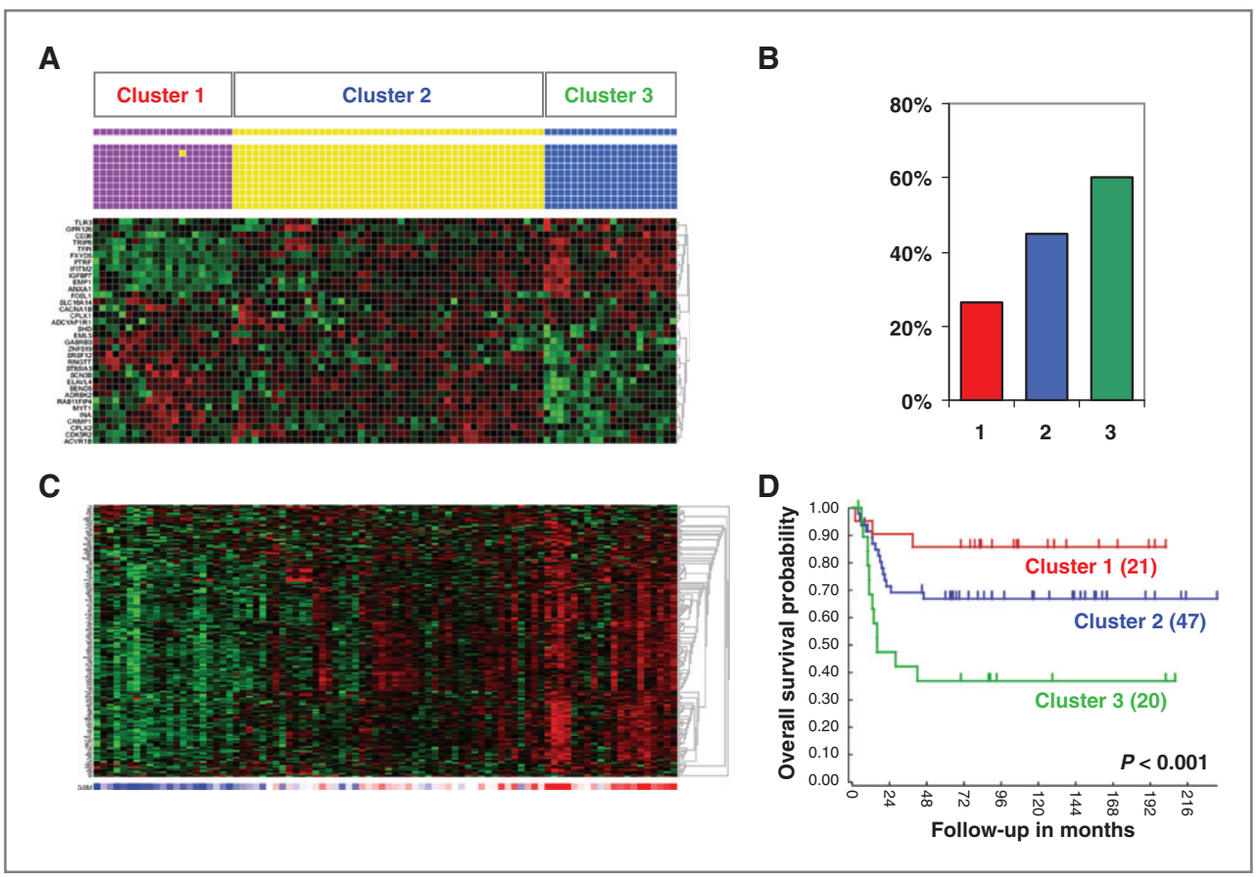

Figure 2. Expression of the migration signature in neuroblastoma correlates with metastatic incidence. A, K-means cluster analysis of 36-gene migration signature in a series of 88 primary neuroblastoma tumors. High and low z-score expression values are indicated in red and green, respectively. Cluster arm assignment for individual tumors in repeated cluster procedures is indicated by yellow, purple, and blue boxes; see main text for detailed explanation. B, frequency of primary tumors with bone and bone marrow metastasis at diagnosis for each K-means cluster as identified in A. C, supervised cluster analysis of a glioblastoma MGES guided by sample order of the K-means clustering in A. D, Kaplan–Meier survival analysis of K-means clusters as identified in A.

expression pattern of the signature genes observed *in vitro* corresponded with the pattern of coregulation *in vivo* (Figs. 1B and 2A). In cluster 3, all (12/12) overexpressed genes in high migration cell lines were upregulated, whereas 20 out of 24 underexpressed genes were downregulated (2-tailed Fisher exact test; $P < 0.001$). The 4 remaining genes were not differentially expressed *in vivo* (Fig. 2A).

Analysis of the clinical parameters showed that the frequency of bone and bone marrow metastasis increased from 26% in cluster 1 to 44% in cluster 2 and 60% in cluster 3 (Fig. 2B). In contrast, the migration signature did not correlate with local invasion of the lymph nodes.

Mesenchymal transformation has been observed in glioblastoma and SCLC (6, 10). We therefore asked whether the neuroblastoma tumors with an active migration signature have an active mesenchymal signature. Gene set enrichment analysis (GSEA) revealed that neuroblastoma tumors with the migration signature were strongly enriched for the glioblastoma mesenchymal gene expression signature (MGES; ref. 7; χ^2; $P < 0.001$). Supervised cluster analysis of the neuroblastoma series for the *MGES* genes showed their expression to strongly correlate with the 36 genes of the migration signature (Fig. 2C). Of note, the migration signature showed a limited overlap of only 3 genes with MGES.

Kaplan–Meier analysis showed that cluster 3 tumors with the high migration signature were associated with the poorest survival, whereas cluster 1 tumors with a low migration signature corresponded to the best survival (log-rank test; $P < 0.001$; Fig. 2D). Supplementary Table S3 shows an evenly distribution of the different neuroblastoma stages over tumors with low, intermediate, or high expression of the migration signature. Thus, characterization of a gene expression signature associated with migratory phenotype identifies a hitherto unspecified group of neuroblastoma tumors with mesenchymal gene expression characteristics, distant mestastases, and poor outcome.

The migration signature identifies a mesenchymal subtype in glioblastoma

Expression profiling of glioblastoma brain tumors identified 3 molecular types: proneural, proliferating, and mesenchymal, the latter correlating with the occurrence of metastasis (6). As a further test whether the 36-gene migration signature relates to mesenchymal characteristics, we analyzed a published series of 284 glioblastoma tumors (21) with a known gene classifier for the 3 molecular subtypes (ref. 6 and see Materials and Methods; Fig. 3A). Tumors of mesenchymal subtype were also active for the

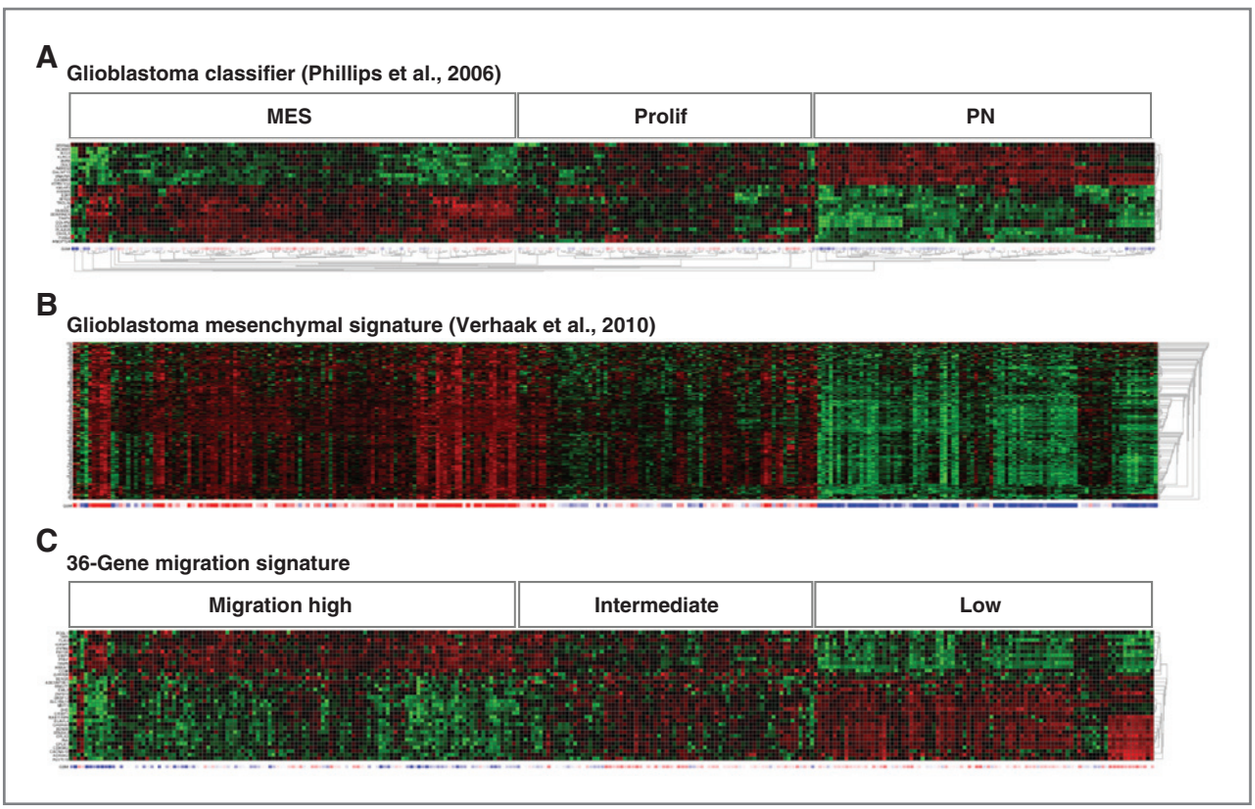

Figure 3. The migration signature is coexpressed with a mesenchymal subtype in glioblastoma. A, unsupervised cluster analysis of 284 glioblastomas in mesenchymal (MES), proliferating (Prolif), and proneural (PN) groups using a glioblastoma classifier signature from (ref. 6). B, supervised cluster analysis of a glioblastoma MGES (7). C, supervised cluster analysis of the neuroblastoma 36-gene migration signature. Tumor groups with predicted high, low, and intermediate migration are indicated. High and low z-score expression values in red and green, respectively. Supervised cluster analysis in B and C use sample order according to clustering shown in A.

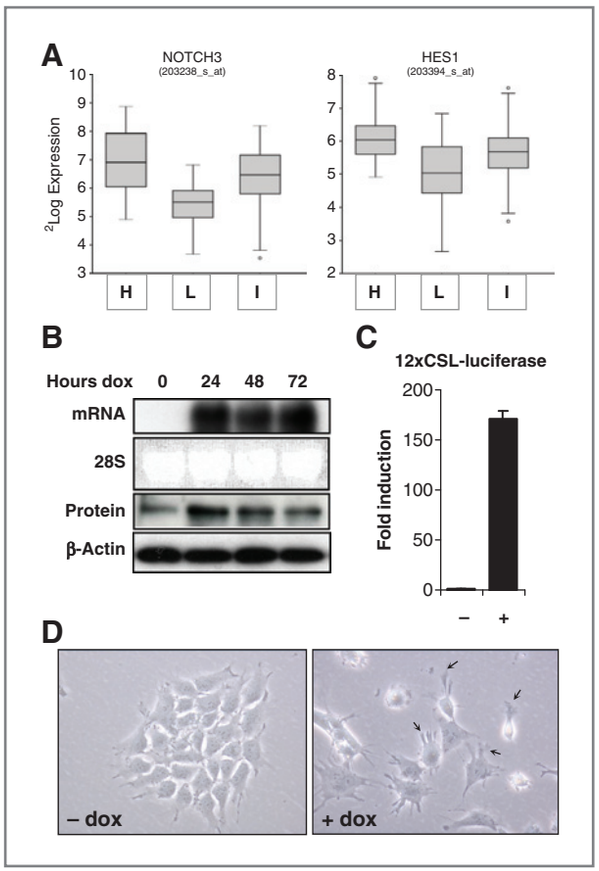

Figure 4. NOTCH3-IC induces a mesenchymal phenotype. A, expression of NOTCH3 and HES1, related to subgroups of low-intermediate-high migration signatures. B, Northern blot analysis of NOTCH3-IC mRNA and Western blot analysis of NOTCH3-IC protein in IMR32 cells at 24, 48, and 72 hours after addition of doxycycline (dox). Note endogenous activation of NOTCH3-IC protein at time-point T = 0. C, analysis of 12xCSL-luciferase NOTCH reporter activity at 48 hours after induction of NOTCH3-IC overexpression. D, morphologic phenotype of IMR32 cells overexpressing NOTCH3-IC (+dox). Arrows indicate outgrowth of lamellipodia-like structures.

independently derived MGES signature (ref. 7; χ^2; $P < 0.001$; Fig. 3B). This clustering in proneural, mesenchymal, and proliferating subtypes (Fig. 3A) was used for a supervised clustering of the expression levels of the 36-gene migration signature. The neuroblastoma migration signature was highly active in glioblastoma of the mesenchymal subtype (GSEA; $P < 0.001$; Fig. 3C). A similar upregulation of the migration signature in glioblastoma of mesenchymal type was identified in an independent series of 395 glioblastoma tumors (ref. 7; Supplementary Fig. S2). We conclude that the 36-gene migration signature identifies glioblastoma tumors of mesenchymal subtype.

NOTCH3-IC induces a highly migratory phenotype in neuroblastoma cells

The identification of neuroblastoma tumors and cell lines with a mesenchymal molecular signature raised the question as to the pathways that control this state. We therefore searched for developmental pathways differentially expressed between neuroblastoma tumors with a high versus low migratory signature (cluster 3 vs. cluster 1). There were 290 genes differentially expressed (ANOVA; $P < 0.01$; FDR-corrected) that were classified to function in development [Gene Ontology (GO) ID 7275]. This list was enriched for genes of the NOTCH pathway as defined by Kyoto Encyclopedia of Genes and Genomes. As Notch3 is expressed in neural crest precursor cells during early mouse development (22), we analyzed whether NOTCH3 expression related to the migration signature. NOTCH3 and HES1 mRNA was upregulated in tumors with a high migration signature (Fig. 4A), and NOTCH3-IC protein was more abundant in high migration cell lines (Supplementary Fig. S3). We therefore functionally tested whether the NOTCH3 transcription factor can induce a migratory phenotype in neuroblastoma cell lines.

Neuroblastoma cell line IMR32 has a low migratory index (Fig. 1A). We generated 2 independent clones with doxycycline-inducible expression of a NOTCH3-IC domain construct (see Materials and Methods). Induction of NOTCH3-IC expression was verified by Northern and Western blot analyses (Fig. 4B) and resulted in approximately 170-fold increased signal of a Notch reporter construct (12xCSL-binding sites coupled to luciferase gene; Fig. 4C). NOTCH3-IC induction resulted in a dramatic change of cell phenotype. Although wild-type IMR32 cells grew in small groups, the NOTCH3-IC–expressing cells grew more scattered and displayed lamellipodia-like outgrowths, a phenotypic hallmark of a mesenchymal state (Fig. 4D). Time-lapse video microscopy showed that IMR32 cells overexpressing NOTCH3-IC became highly motile, in contrast to control cells (Fig. 5A and Supplementary videos S1 and S2). Also a scratch assay for cell migration showed that IMR32 cells overexpressing NOTCH3-IC migrated significantly faster into the wounded area compared with IMR32 control cells (Student t test; $P = 0.018$; Fig. 5B). In Transwell migration assays, NOTCH3-IC induced migration approximately 10-fold (Student t test; $P < 0.001$; Fig. 5C). To confirm the function of NOTCH3-IC in migration, we introduced the doxycycline-inducible NOTCH3-IC expression vector in neuroblastoma cell line SK-N-BE (Supplementary Fig. S4A). Like in IMR32, NOTCH3-IC induced migration of SK-N-BE cells (Supplementary Fig. S4B). In a complementary approach, we tested whether *NOTCH3* was required for the high migration phenotype in SH-EP2. Isopropyl-beta-D-thiogalactoside (IPTG) inducible expression of NOTCH3 short hairpin RNAs reduced NOTCH3 protein expression and attenuated migration of SH-EP2 cells (Supplementary Fig. S5A and S5B). We conclude that NOTCH3-IC induces an extremely strong migratory phenotype as well as changes in cell morphology reminiscent of a mesenchymal state.

NOTCH3-IC induces mesenchymal marker gene expression in neuroblastoma cells

We studied the NOTCH3 downstream pathway by microarray mRNA profiling of time series of both IMR32 clones

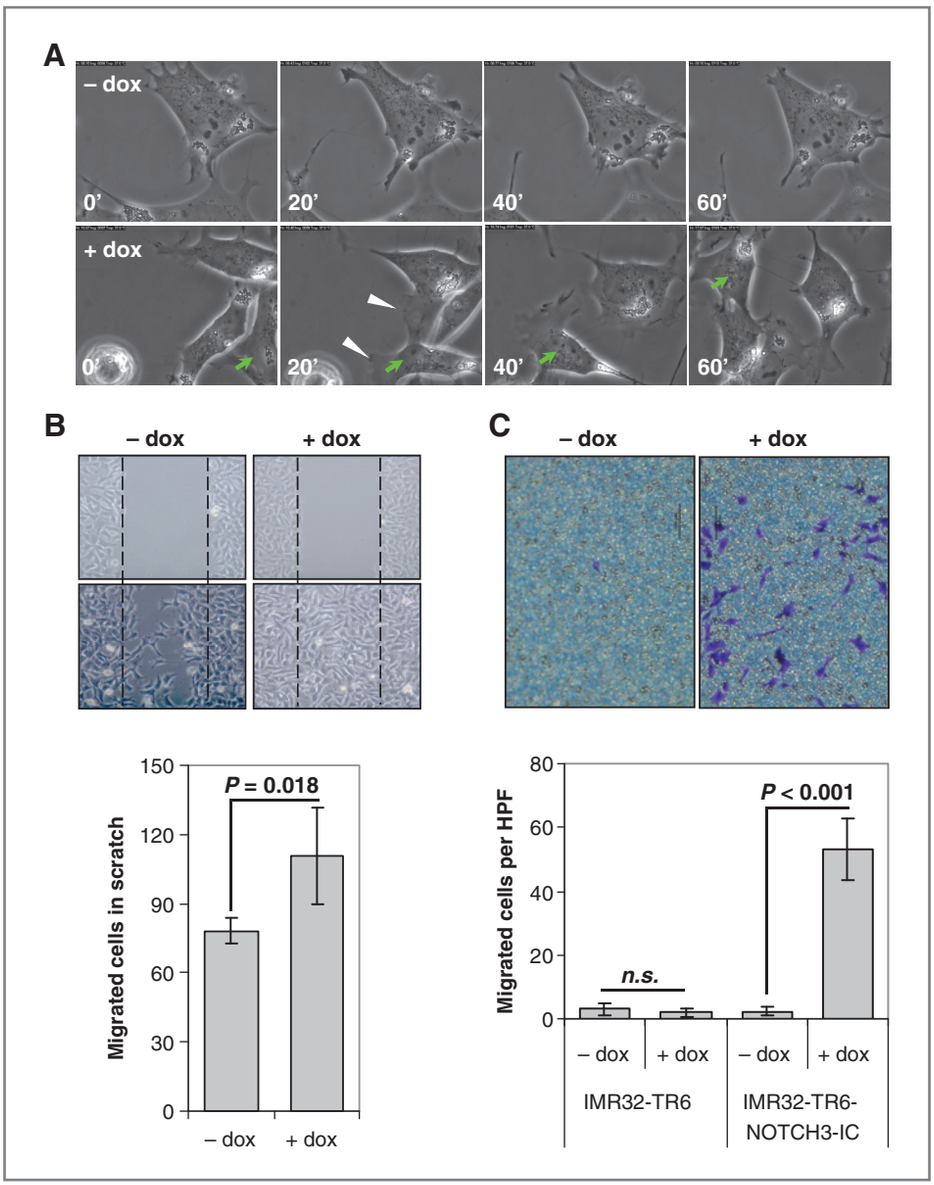

Figure 5. Expression of NOTCH3-IC induces cell motility. A, snapshot images from 20-minute intervals in time-lapse imaging. Green arrow indicates strong induction of migratory behavior of a single cell with NOTCH3-IC induction. Note lamellipodia at the leading edge (white arrowheads). B, wound-healing assay of NOTCH3-IC overexpressing cells. Bottom, quantification of migrated cells into scratch. C, representative brightfield pictures of Transwell migration assay. Migrated cells are stained with crystal violet. Bottom, quantification of Transwell migration assay. n.s., not significant

with NOTCH3-IC overexpression (see Materials and Methods). Eight time-points from 0 to 120 hours postinduction were analyzed. At a cut-off level of ^{2}logfold more than 1 regulation, 447 genes were significantly upregulated and 61 genes downregulated (Supplementary Table S1). At a cut-off level of more than 2, there were 187 genes upregulated and only 2 genes downregulated (Supplementary Table S1). The target gene list included known NOTCH transcriptional targets from the HES and HEY families (Supplementary Table S5).

GO analysis of regulated genes (^{2}logfold >1) revealed enriched categories ($P < 0.001$) of "tissue remodeling" (18 genes), "localization of cell" (64 genes), "cell adhesion" (52 genes), and "regulation of locomotion" (22 genes), confirming that NOTCH3 regulates a gene expression programme associated with cell migration. We conclude that NOTCH3-IC functions as a master switch in IMR32 that induces a large set of cell motility genes and confers a motile phenotype to the cells. To test whether this is also a function of NOTCH3 in neuroblastoma tumors, we analyzed the expression of the NOTCH3 target genes in the AMC-NB88 series. Differential gene expression analysis between high and low migration signature subgroups revealed that NOTCH3-IC target genes (^{2}logfold >2 regulation) were strongly enriched in the high migration subgroup (χ^2; $P < 0.001$; Fig. 6A).

Consistent with the induction of a mesenchymal-like morphology, NOTCH3-IC induced the expression of mesenchymal marker genes, for example, smooth muscle actin (SMA; encoded by ACTA2), fibronectin (FN1), SPARC,

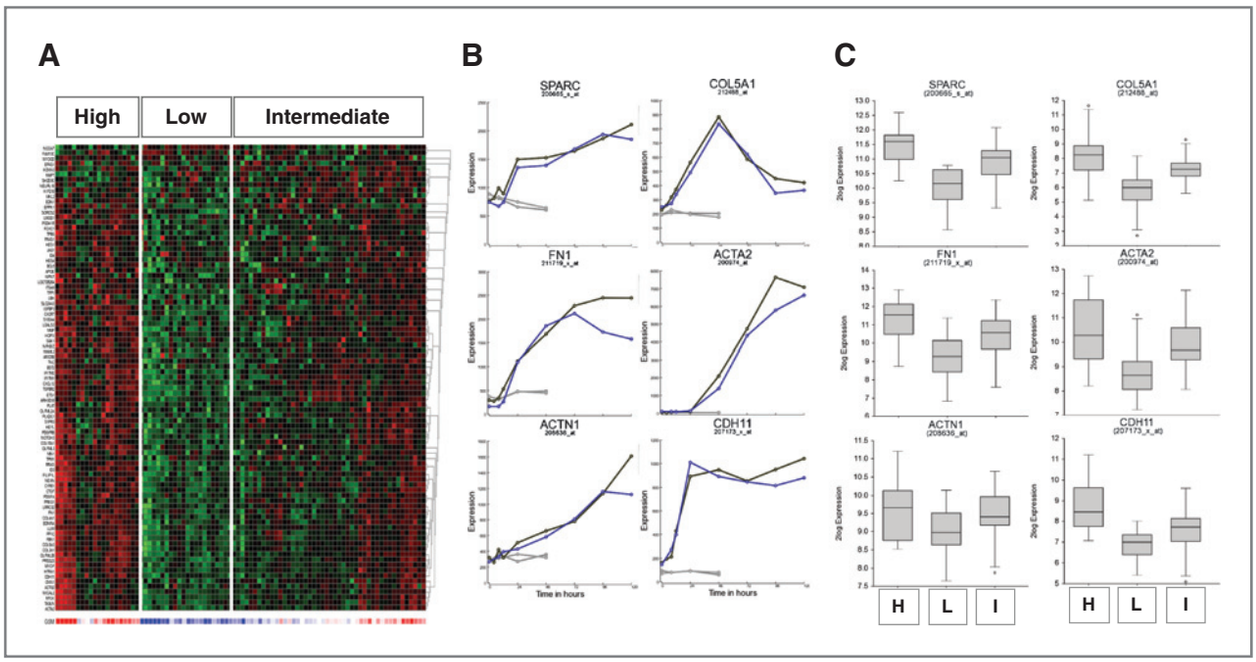

Figure 6. NOTCH3-IC target gene signature includes mesenchymal marker genes and is upregulated in neuroblastoma tumors of mesenchymal subtype. A, supervised cluster analysis of a NOTCH3-IC target gene signature in subgroups of high, low, and intermediate migration. B, induction of mesenchymal marker genes SPARC, FN1, ACTN1, COL5A1, ACTA2, and CDH11 by NOTCH3-IC. Expression values from 2 independent IMR32-TR6-NOTCH3-IC clones (clone 6 in blue and 8 in black) and 2 parental IMR32-TR6 clones (in grey) are shown on the *y*-axis. Time (h) after NOTCH3-IC induction is on the *x*-axis. C, expression of mesenchymal marker genes SPARC, FN1, ACTN1, COL5A1, ACTA2, and CDH11 in subgroups of high, low, and intermediate (indicated H, L, I, respectively) migration tumors.

ACTN1, COL5A1, and CDH11 in IMR32 (Fig. 6B). These mesenchymal markers were upregulated in AMC-NB88 tumors expressing the high migration signature (Fig. 6C). Similar findings were observed in 2 independent neuroblastoma tumor series (ref. 23; $n = 50$; ref. 24; $n = 101$; Supplementary Fig. S6). Thus, NOTCH3-IC induces morphologic features and a mesenchymal marker gene profile suggesting a mesenchymal-like reprogramming of IMR32 neuroblastoma cells.

A NOTCH3-IC signature is coordinately expressed in a wide range of tumor types

Although motility is a tightly controlled phenotype with a major impact on normal development and cancer and the Notch pathway is active in many tissues, we asked whether NOTCH3 governs a motility pathway in other tumor types as well. We analyzed the 447 genes that were induced by NOTCH3 in neuroblastoma cells for correlation with NOTCH3 expression in published series of other human tumor types. We investigated tumor series of colon (ref. 25; $n = 232$), kidney (Expression Project for Oncology; expO; $n = 261$), ovary (expO; $n = 256$), and breast (expO; $n = 351$). Each of the series included samples with substantial NOTCH3 expression. Strikingly, a large fraction of the 447 genes induced by NOTCH3-IC *in vitro* strongly correlated to NOTCH3 expression in all analyzed tumor types. In colon tumors, expression of 237 genes (53%) significantly correlated to NOTCH3 expression (^{2}log Pearson correlation; $P < 0.01$). Similar numbers were found in kidney cancer (249 genes, 55%), breast cancer (176 genes, 39%), and slightly lower numbers in ovarian cancer (121 genes, 27%). Visualization of NOTCH3-IC target genes by K-means cluster analysis revealed strongly coregulated patterns of expression (Supplementary Fig. S7A–S7D). This strongly suggests that a NOTCH3-regulated gene module controlling motility in neuroblastoma is active in a wide range of human tumor types.

Discussion

High-stage neuroblastoma is characterized by widespread metastasis to bone and bone marrow contributing to extremely poor outcome. However, the molecular master switches that control motility and invasion of neuroblastoma have remained largely unknown. We characterized the migration indices of a neuroblastoma cell line panel as a functional exponent of a mesenchymal phenotype. This yielded a 36-gene migration signature that correctly predicted cell migration in cell lines of various tumor backgrounds (Fig. 1). Functional gene expression signatures obtained in cell line studies have previously allowed classification of human tumor series (26). The 36-gene migration signature identified a group of neuroblastoma tumors characterized by an increased metastatic incidence and poor survival.

The metastatic potential of tumors has been associated with a mesenchymal phenotype. This was, for example,

observed in gene expression profiles of glioblastoma series where the mesenchymal subtype corresponded with invasive tumors (6, 7). We observed that this mesenchymal subtype of glioblastoma was also positive for the 36-gene motility signature identified in neuroblastoma. Accordingly, a mesenchymal signature established for glioblastoma identified the neuroblastoma tumors positive for the motility signature. These data suggest that a subset of neuroblastoma tumors has mesenchymal characteristics because they show an increased incidence of metastases and an upregulation of genes from the migration signature and a mesenchymal signature (MGES; Figs. 2 and 6).

Bioinformatic analysis suggested that NOTCH signaling was associated with this mesenchymal subtype of neuroblastoma tumors. Induced expression of a NOTCH3-IC transgene in IMR32 neuroblastoma cells indeed conferred a series of mesenchymal hallmarks: strongly increased motility, lamellipodia-like outgrowths, and mesenchymal marker gene expression (Figs. 4–6). Surprisingly, the *NOTCH3* gene expression module identified in neuroblastoma was also recognized in a wide range of other tumor types. This implies that gene expression profiles can be deconstructed in modular functional groups when the "master gene" is known (Supplementary Fig. S7).

NOTCH signaling has been previously implicated in neuroblastoma. Overexpression of each of the NOTCH-IC paralogues inhibited neuroblastoma growth (27). In our experiments, NOTCH3-IC induces cell motility (Fig. 5) as well as a transient attenuation of the cell cycle (data not shown). Thus, it might be that tumor aggressiveness can be achieved by increased motility but at the cost of a temporarily decrease in proliferation rate. Although we identify NOTCH3 as a master switch for cell motility, the detailed executioners of this phenotype remain to be investigated. As NOTCH3-IC induced a series of classical NOTCH target genes from HES and HEY families in IMR32 that also correlate with NOTCH3 expression in neuroblastoma tumors, we expect much of the here established NOTCH3-IC downstream signature as directly or indirectly regulated target genes responsible for cell migration. In agreement with an aggressive function of NOTCH signaling in neuroblastoma, high levels of NOTCH1 protein predicted a poor prognosis in neuroblastoma (28). Inhibition of γ-secretase activity, required for NOTCH activation, attenuated neuroblastoma cell growth *in vitro* (29) and *in vivo* (28).

We conclude that our integrated approach of wet lab experimental data, human tumor series, and bioinformatic analysis identified a mesenchymal state in neuroblastoma tumors and implicate NOTCH3 as a master regulator of mesenchymal transformation and motility gene expression in neuroblastoma.

Disclosure of Potential Conflicts of Interest

No potential conflicts of interest were disclosed.

Authors' Contributions

Conception and design: J. van Nes, R. Versteeg
Acquisition of data (provided animals, acquired and managed patients, provided facilities, etc.): J. van Nes, A. Chan, T. van Groningen
Analysis and interpretation of data (e.g., statistical analysis, biostatistics, computational analysis): J. van Nes, A. Chan, T. van Groningen, J. Koster
Writing, review, and/or revision of the manuscript: J. van Nes, R. Versteeg
Administrative, technical, or material support (i.e., reporting or organizing data, constructing databases): P. van Sluis
Study supervision: J. van Nes, R. Versteeg

Acknowledgments

The authors thank Jan Stap for help with time-lapse microscopy.

Grant Support

This work was supported by Stichting Kinderen Kankervrij (KiKa) to J. van Nes and R. Versteeg, Tom Voûte Fund to R. Versteeg, and Netherlands Cancer Foundation to T. van Groningen.

The costs of publication of this article were defrayed in part by the payment of page charges. This article must therefore be hereby marked *advertisement* in accordance with 18 U.S.C. Section 1734 solely to indicate this fact.

Received September 20, 2012; revised April 2, 2013; accepted April 25, 2013; published OnlineFirst May 6, 2013.

References

1. Brodeur GM. Neuroblastoma: biological insights into a clinical enigma. Nat Rev Cancer 2003;3:203–16.
2. Sauka-Spengler T, Bronner-Fraser M. A gene regulatory network orchestrates neural crest formation. Nat Rev Mol Cell Biol 2008;9:557–68.
3. Pattyn A, Morin X, Cremer H, Goridis C, Brunet JF. The homeobox gene Phox2b is essential for the development of autonomic neural crest derivatives. Nature 1999;399:366–70.
4. Betancur P, Bronner-Fraser M, Sauka-Spengler T. Assembling neural crest regulatory circuits into a gene regulatory network. Annu Rev Cell Dev Biol 2010;26:581–603.
5. Jiang M, Stanke J, Lahti JM. The connections between neural crest development and neuroblastoma. Curr Top Dev Biol 2011;94:77–127.
6. Phillips HS, Kharbanda S, Chen R, Forrest WF, Soriano RH, Wu TD, et al. Molecular subclasses of high-grade glioma predict prognosis, delineate a pattern of disease progression, and resemble stages in neurogenesis. Cancer Cell 2006;9:157–73.
7. Verhaak RG, Hoadley KA, Purdom E, Wang V, Qi Y, Wilkerson MD, et al. Integrated genomic analysis identifies clinically relevant subtypes of glioblastoma characterized by abnormalities in PDGFRA, IDH1, EGFR, and NF1. Cancer Cell 2010;17:98–110.
8. Carro MS, Lim WK, Alvarez MJ, Bollo RJ, Zhao X, Snyder EY, et al. The transcriptional network for mesenchymal transformation of brain tumours. Nature 2010;463:318–25.
9. Bhat KP, Salazar KL, Balasubramaniyan V, Wani K, Heathcock L, Hollingsworth F, et al. The transcriptional coactivator TAZ regulates mesenchymal differentiation in malignant glioma. Genes Dev 2011;25:2594–609.
10. Calbo J, van ME, Proost N, van DE, Beverloo HB, Meuwissen R, et al. A functional role for tumor cell heterogeneity in a mouse model of small cell lung cancer. Cancer Cell 2011;19:244–56.
11. Scheel C, Eaton EN, Li SH, Chaffer CL, Reinhardt F, Kah KJ, et al. Paracrine and autocrine signals induce and maintain mesenchymal and stem cell states in the breast. Cell 2011;145:926–40.

12. Guo D, Xu BL, Zhang XH, Dong MM. Cancer stem-like side population cells in the human nasopharyngeal carcinoma cell line cne-2 possess epithelial mesenchymal transition properties in association with metastasis. Oncol Rep 2012;28:241–7.
13. Louvi A, Artavanis-Tsakonas S. Notch signalling in vertebrate neural development. Nat Rev Neurosci 2006;7:93–102.
14. Nam Y, Sliz P, Song L, Aster JC, Blacklow SC. Structural basis for cooperativity in recruitment of MAML coactivators to Notch transcription complexes. Cell 2006;124:973–83.
15. Valastyan S, Weinberg RA. Tumor metastasis: molecular insights and evolving paradigms. Cell 2011;147:275–92.
16. Clark EA, Golub TR, Lander ES, Hynes RO. Genomic analysis of metastasis reveals an essential role for RhoC. Nature 2000;406:532–5.
17. Gobeil S, Zhu X, Doillon CJ, Green MR. A genome-wide shRNA screen identifies GAS1 as a novel melanoma metastasis suppressor gene. Genes Dev 2008;22:2932–40.
18. Ino Y, Gotoh M, Sakamoto M, Tsukagoshi K, Hirohashi S. Dysadherin, a cancer-associated cell membrane glycoprotein, down-regulates E-cadherin and promotes metastasis. Proc Natl Acad Sci U S A 2002;99:365–70.
19. Shimamura T, Yasuda J, Ino Y, Gotoh M, Tsuchiya A, Nakajima A, et al. Dysadherin expression facilitates cell motility and metastatic potential of human pancreatic cancer cells. Cancer Res 2004;64:6989–95.
20. de Graauw M, van Miltenburg MH, Schmidt MK, Pont C, Lalai R, Kartopawiro J, et al. Annexin A1 regulates TGF-beta signaling and promotes metastasis formation of basal-like breast cancer cells. Proc Natl Acad Sci U S A 2010;107:6340–5.
21. Gravendeel LA, Kouwenhoven MC, Gevaert O, de Rooi JJ, Stubbs AP, Duijm JE, et al. Intrinsic gene expression profiles of gliomas are a better predictor of survival than histology. Cancer Res 2009; 69:9065–72.
22. Williams R, Lendahl U, Lardelli M. Complementary and combinatorial patterns of Notch gene family expression during early mouse development. Mech Dev 1995;53:357–68.
23. Fix A, Lucchesi C, Ribeiro A, Lequin D, Pierron G, Schleiermacher G, et al. Characterization of amplicons in neuroblastoma: high-resolution mapping using DNA microarrays, relationship with outcome, and identification of overexpressed genes. Genes Chromosomes Cancer 2008;47:819–34.
24. Wang Q, Diskin S, Rappaport E, Attiyeh E, Mosse Y, Shue D, et al. Integrative genomics identifies distinct molecular classes of neuroblastoma and shows that multiple genes are targeted by regional alterations in DNA copy number. Cancer Res 2006;66: 6050–62.
25. Smith JJ, Deane NG, Wu F, Merchant NB, Zhang B, Jiang A, et al. Experimentally derived metastasis gene expression profile predicts recurrence and death in patients with colon cancer. Gastroenterology 2010;138:958–68.
26. Chang HY, Nuyten DS, Sneddon JB, Hastie T, Tibshirani R, Sorlie T, et al. Robustness, scalability, and integration of a wound-response gene expression signature in predicting breast cancer survival. Proc Natl Acad Sci U S A 2005;102:3738–43.
27. Zage PE, Nolo R, Fang W, Stewart J, Garcia-Manero G, Zweidler-McKay PA. Notch pathway activation induces neuroblastoma tumor cell growth arrest. Pediatr Blood Cancer 2012;58:682–9.
28. Chang HH, Lee H, Hu MK, Tsao PN, Juan HF, Huang MC, et al. Notch1 expression predicts an unfavorable prognosis and serves as a therapeutic target of patients with neuroblastoma. Clin Cancer Res 2010;16:4411–20.
29. Ferrari-Toninelli G, Bonini SA, Uberti D, Buizza L, Bettinsoli P, Poliani PL, et al. Targeting Notch pathway induces growth inhibition and differentiation of neuroblastoma cells. Neuro Oncol 2010;12:1231–43.
30. Saeed AI, Sharov V, White J, Li J, Liang W, Bhagabati N, et al. TM4: a free, open-source system for microarray data management and analysis. Biotechniques 2003;34:374–8.
31. Saeed AI, Bhagabati NK, Braisted JC, Liang W, Sharov V, Howe EA, et al. TM4 microarray software suite. Methods Enzymol 2006;411: 134–93.